A Novel Conceptual Design by Integrating NGL Recovery and LNG Regasification Processes for Maximum Energy Savings

Meiqian Wang, Jian Zhang, and Qiang Xu
Dan F. Smith Dept. of Chemical Engineering, Lamar University, Beaumont, TX 77710

DOI 10.1002/aic.14231
Published online October 30, 2013 in Wiley Online Library (wileyonlinelibrary.com)

Natural gas liquids (NGL) recovery from shale gas needs large amounts of cold energy for cooling, while liquefied natural gas (LNG) regasification requires tremendous hot energy for heating. Thus, recycling the cold energy from LNG regasification process at a receiving terminal to assist the NGL recovery process has great economic benefits on both energy saving and high-value product recovery. A novel conceptual design by integrating NGL recovery from shale gas and LNG regasification at receiving terminals has been developed. It first generates a process superstructure. Then, a simulation-assisted mixed-integer linear programming (MILP) model is developed and solved for the optimal process synthesis. Next, heat exchange network (HEN) design and analysis are performed to accomplish the maximum energy-saving target. Finally, rigorous plant-wide simulations are conducted to validate the feasibility and capability of the entire conceptual design coupling of separation and heat integration. © 2013 American Institute of Chemical Engineers
AIChE J, 59: 4673–4685, 2013
Keywords: shale gas, NGL recovery, LNG regasification, process design and synthesis, MILP

Introduction

Natural gas is an important clean energy source to sustain human civilization in this century. It is reported that the US natural gas reserves which can be technically recovered are 2,587 Tcf (trillion cubic feet).[1] These include undiscovered, unproved, and unconventional natural gases, which can significantly change future energy supply and consumption markets in the US, or even the world. According to a statistical review,[2] the global natural gas production increased by 3.1% in 2011; in the meantime, the global natural gas trade increased by a relatively modest 4% and liquefied natural gas (LNG) shipments climbed up by 10.1%.

Shale gas, a type of natural gas formed and trapped within shale formation, becomes an increasingly important player in the natural gas family. In the past decades, technological advancements such as hydraulic fracturing and horizontal drilling have successfully made natural gas extraction from deep underground shale rock formations viable and profitable.[3] This booms shale gas production at a rapid speed, accounting for about 20% share of the total US onshore domestic natural gas production in 2010. EIA forecasts that shale gas can even possibly account for over 50% of onshore natural gas production by 2035.[4] Normally, shale gas contains valuable heavy hydrocarbons such as ethane, propane, butane, and pentanes. These hydrocarbons can be recovered as natural gas liquids (NGL) through cryogenic separation processes. The purpose of NGL recovery is obvious: the heavy components have much higher market values than methane, the majority of natural gas, which is mainly used as a fuel gas. Due to the large quantities of shale gas processed nationally and internationally, NGL recovery can be very profitable for oil and gas industries; besides, those recovered heavy components such as ethane and propane are very important feed stocks that can significantly benefit downstream petrochemical/chemical industries.

Cryogenic separation is an effective way for NGL recovery, which generally employs a refrigeration system to partially liquefy natural gas before feeding a fractionation process. Conceivably, a cryogenic separation process consumes lots of cold energy for partial liquefaction as well as some hot utilities for the fractionation process. Hence, energy consumption minimization is the major concern for NGL recovery. Unfortunately, effective and efficient technologies for NGL recovery from shale gas have not been adequately addressed.

Figure 1 shows the geographical distribution of shale plays in the US.[5] Interestingly, when it is compared with the distribution of the US LNG receiving terminals shown in Figure 2[6] one can easily find that several major shale plays are actually very close to some LNG receiving terminals, especially those near the Gulf Coast and East Coast areas. LNG receiving terminals play an important role in the LNG value chain, as they receive LNG from oversea/domestic tankers, house LNG in special storage tanks, and subsequently vaporize LNG and deliver natural gas to downstream industrial and residential consumers although pipeline network systems.

Figure 3 provides the sketch of a regular receiving terminal:[7] LNG is stored and shipped in a vessel at the condition of -162°C in temperature and 0.108 MPa in pressure. When the vessel arrives at a receiving terminal, LNG is first unloaded to onshore LNG storage tanks. Later on, the LNG

Correspondence concerning this article should be addressed to Q. Xu at Qiang.xu@lamar.edu).

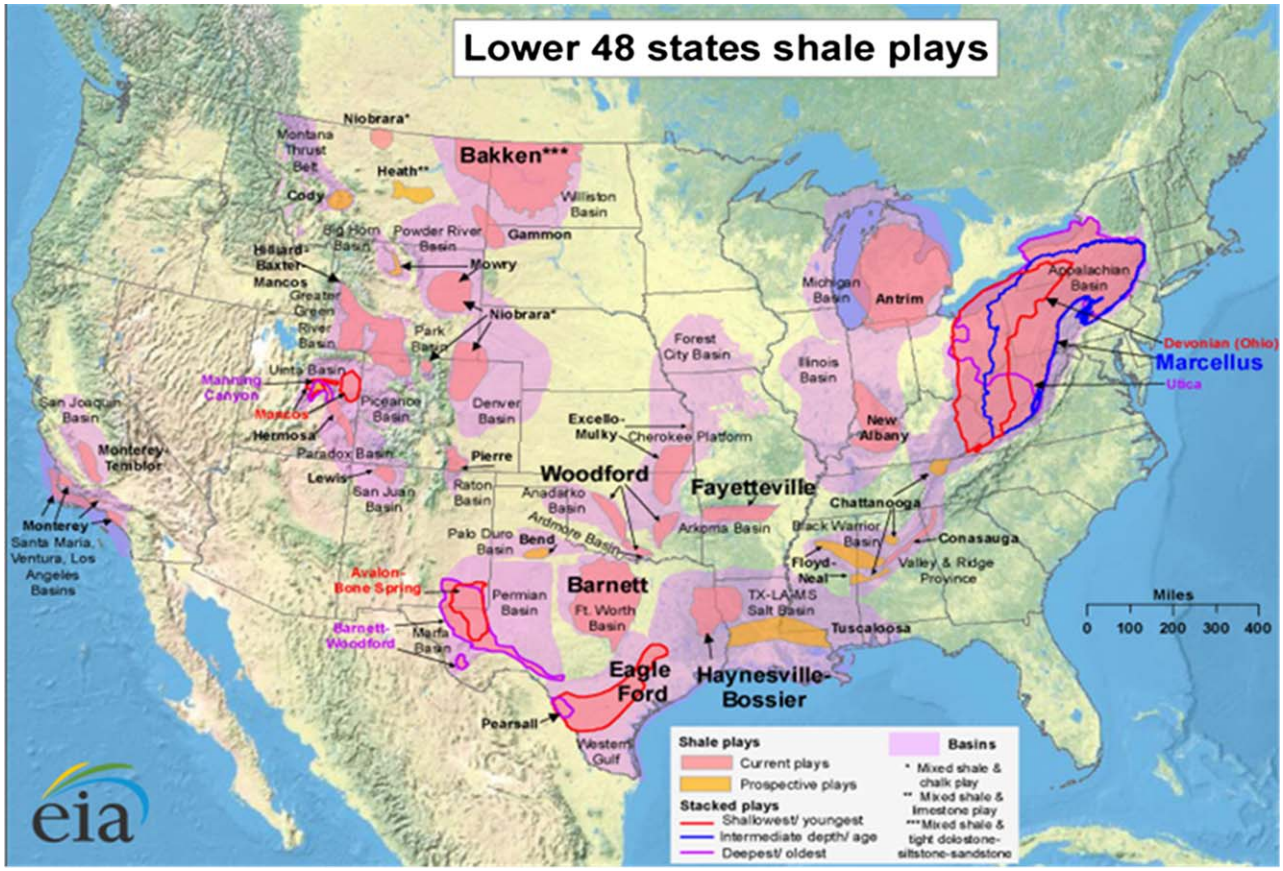

Figure 1. Shale plays distribution in the US.[5]

[Color figure can be viewed in the online issue, which is available at wileyonlinelibrary.com.]

is sent out by several in-tank pumps, by which the LNG pressure is increased to about 7 MPa. Next, the high-pressure LNG is sent to a vaporizer, where it will be fully evaporated so that it can be sent to electricity generation facilities or local customers through downstream pipeline networks.

It should be highlighted that during the LNG regasification process, tremendous amounts of hot energy will be consumed for the vaporization operation. In other words, the cold energy from LNG regasification must be dumped to some hot sinks. The most common heating sources for LNG vaporization are seawater and/or combustion of natural gas itself. In this way, apparently, tremendous amounts of cold energy from LNG and valuable natural gas is wasted; meanwhile, negative environmental impacts, such as local seawater temperature increase and air emissions, are also induced.

Note that NGL recovery from shale gas needs very large amounts of cold energy for cooling, while LNG regasification requires tremendous hot energy for heating. If these two processes could be integrated at those receiving terminals geographically close to shale plays, cold energy recycled from the LNG regasification process can be effectively used to assist the NGL recovery process, which accomplishes a win-win situation by exchanging both available hot and cold energy internally, thus, results in great economic benefits on energy savings. Furthermore, the LNG to be regasified contains some heavy components as well, which can also be recovered when an NGL recovery process is integrated. Table 1 gives a typical composition distribution of LNG, showing about 8 wt % of LNG may be recovered as NGL. Therefore, the integration of NGL recovery for shale gas with LNG regasification at receiving terminals can generate considerable economic benefits on high-value product recovery as well.

At LNG receiving terminals, NGL recovery is usually conducted after LNG vaporization and processed in subsequent traditional gas plants. Only a few references from the oil and gas industry addressed the combination of NGL recovery processes with LNG re-gasification processes.[8,9] Through this integration, their processes were claimed for saving work from gas compression and taking advantage of using the cold energy from LNG. Cuellar et al.[10] pointed out another advantage of this integration to be that the delivered heating value can be controlled through NGL recovering. However, based on the available literature survey, there is still a lack of systematic studies on the integration of NGL recovery from shale gas and LNG regasification at receiving terminals. The heat-integrated process design and operation for simultaneous energy saving and NGL recovery optimization has never been reported.

In this article, a novel conceptual design by integrating shale gas NGL recovery with LNG regasification (SRR) at receiving terminals has been developed. First, four alternative operating conditions are considered at each separation stage based on industrial experiences as well as lots of simulations. All of the considered operating conditions form a process superstructure. A simulation-assisted mixed-integer linear programming (MILP) model is then developed and

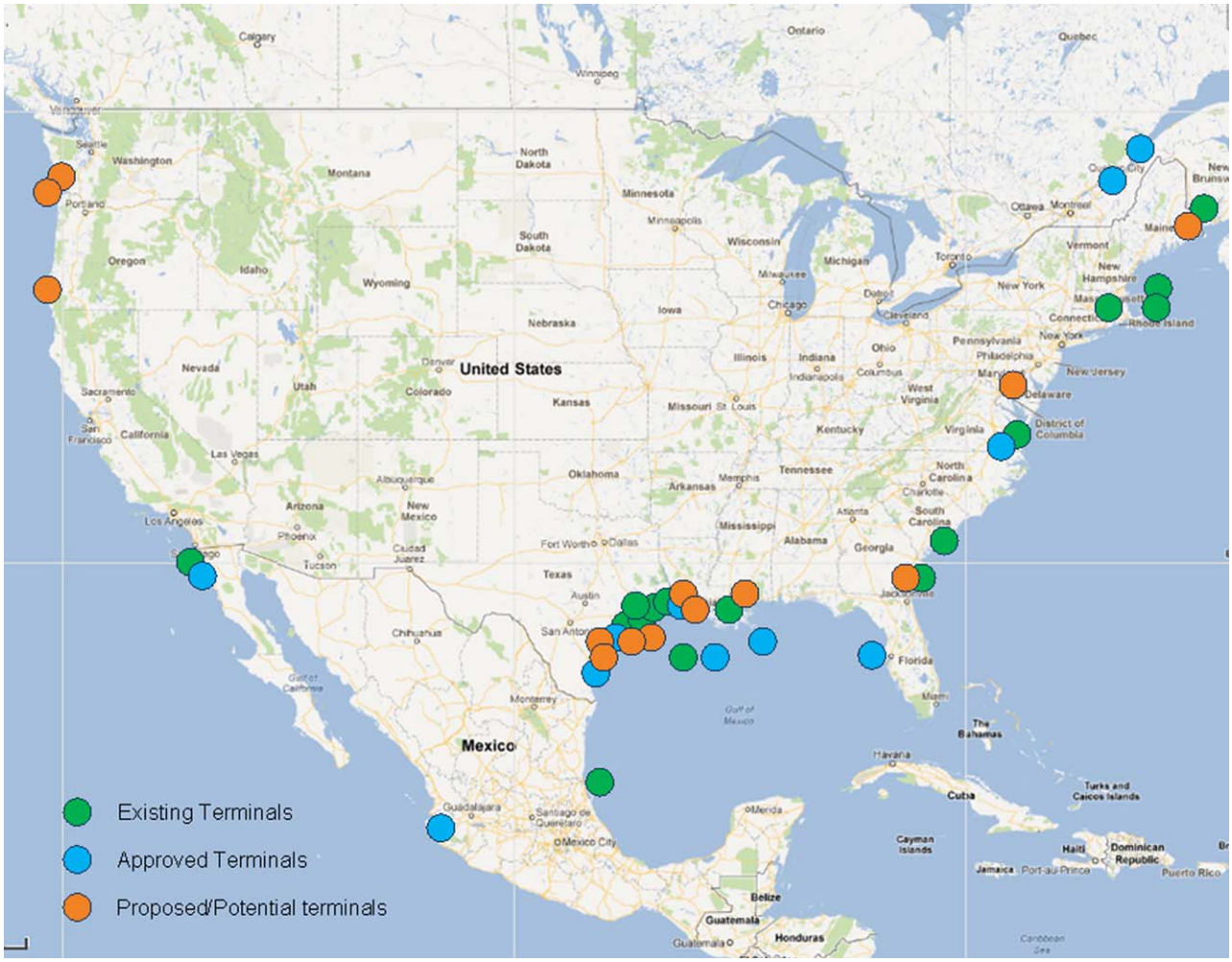

Figure 2. Existing and proposed LNG receiving terminals in the US.[6]

[Color figure can be viewed in the online issue, which is available at wileyonlinelibrary.com.]

solved for the optimal synthesis. Second, heat exchange network (HEN) design and analysis are performed to accomplish the maximum energy-saving target. Finally, rigorous plant-wide simulations are conducted to validate the feasibility and capability of the entire conceptual design coupling of separation and heat integration. This case study has demonstrated the efficacy of the conceptual design and its salient application potentials.

General Methodology Framework

As indicated in Figure 4, the general methodology framework of this study includes four major steps of work.

The first step is to develop the superstructure for an SRR process at the receiving terminal. The main idea is through energy integration among all the possible process streams to minimize the utility cost (high-pressure steam, low-pressure steam, water, and electricity) while making more NGL

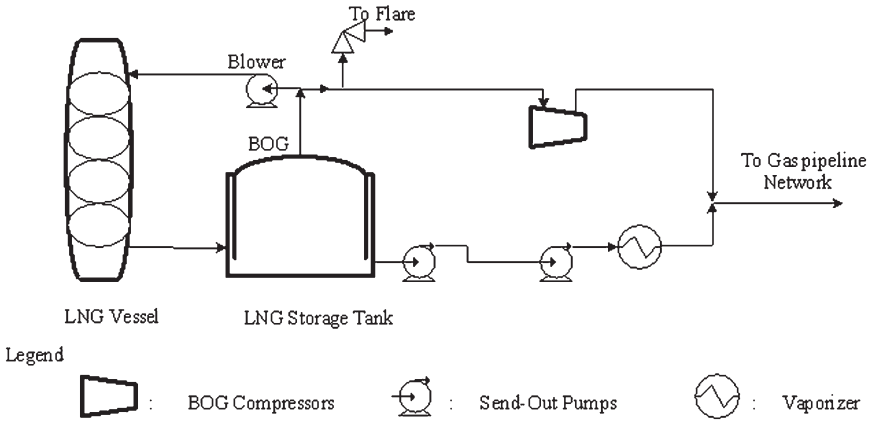

Figure 3. Sketch of a regular LNG receiving terminal.[7]

Table 1. Typical Composition of an LNG Stream

Component	Composition (wt %)
Nitrogen	1.00
Methane	90.97
Ethane	6.00
Propane	1.50
Isobutane	0.30
n-Butane	0.20
Isopentane	0.01
n-Pentane	0.02

products from shale gas and LNG streams. Figure 5 shows the sketch of the proposed SRR process. The four major units involved in the NGL recovery process are scrubber, deethanizer (DeC2), depropanizer (DeC3), and debutanizer (DeC4). After passing through several units, such as pump, heat exchanger, or compressor, LNG and shale gas are mixed and sent to a scrubber. The scrubber top stream, which mainly contains methane, is the natural gas product. Additional processing is still needed to increase the pressure of natural gas product to 7 MPa, and raise its temperature to 4°C before sent to the pipeline system. Ethane and other heavier compounds from the bottom of scrubber are sequentially separated although DeC2, DeC3, and DeC4.

For each column, four alternative operating conditions are considered, which would give a total of 256 different operation combinations. Some units, such as column, pump or compressor, involve a lot of complicated thermodynamic functions, which are hard to solve in a single optimization model. Hence, each column operating conditions is actually simulated individually in advance via Aspen Plus[11] according to their product specifications, instead of developing rigorous unit models and solving them in one optimization model. Peng-Robinson equation of state is used as the thermodynamic property method for simulation, because it is recommended for gas processing, refinery, and petrochemical applications.[11] Note that each column operating condition has to be simulated separately because the total combinational scenarios would be too many when all four stages of separations are considered together. To keep the consistency, the top and bottom streams of four alternative states for one column is assumed to have the same composition and flow rate specifications but different temperatures and

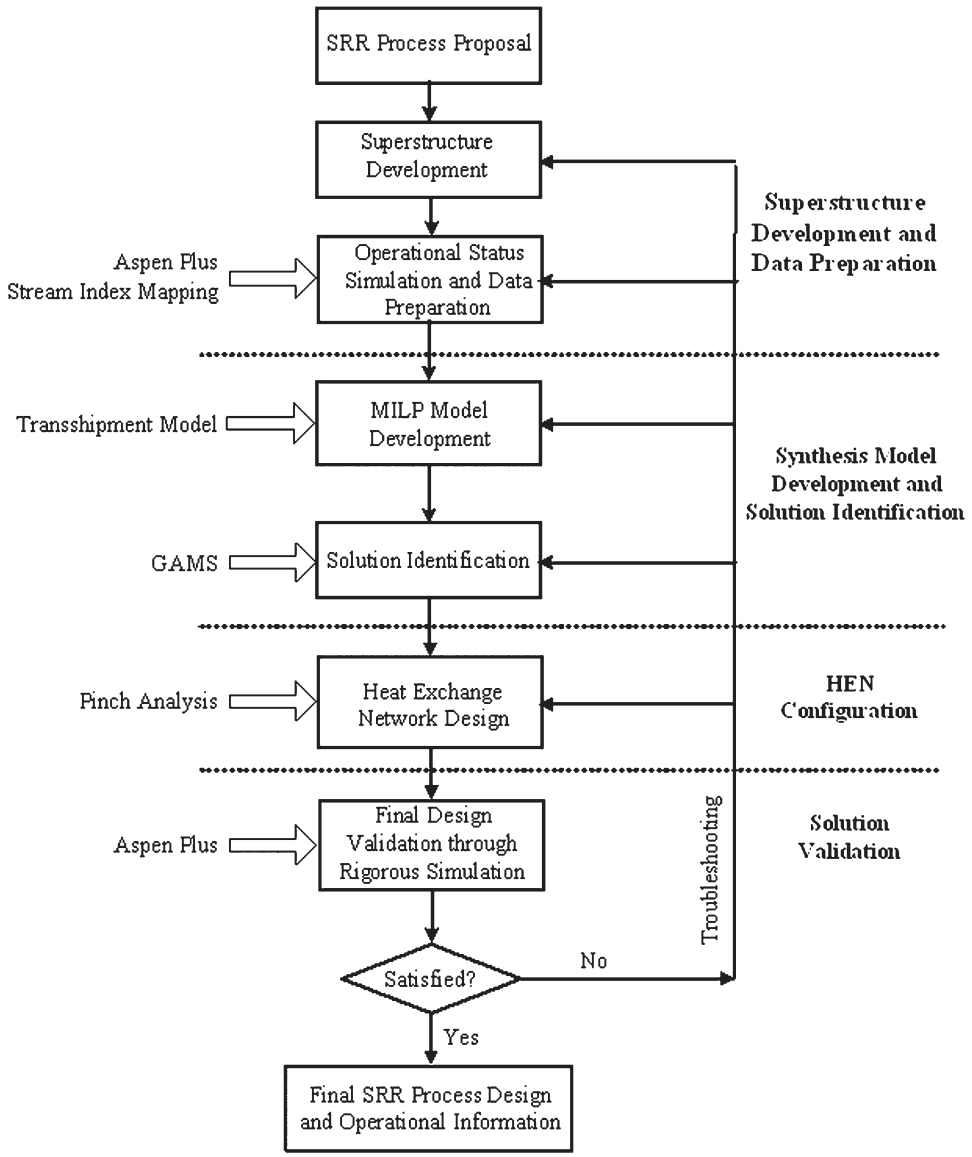

Figure 4. General methodology framework.

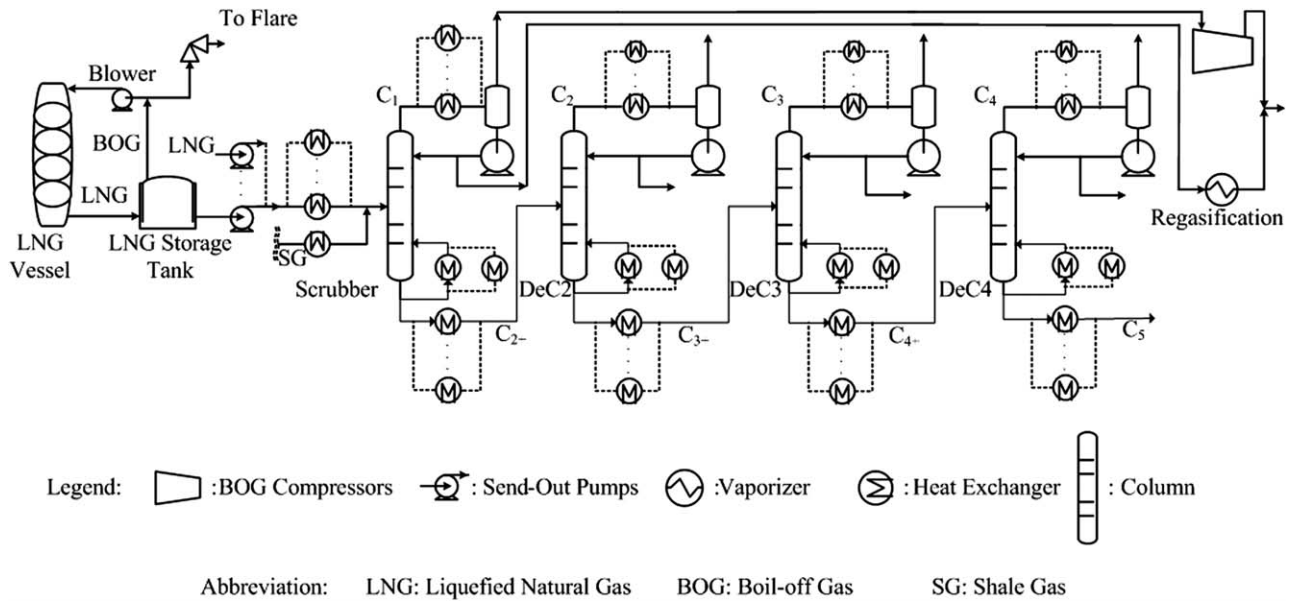

Figure 5. Sketch of the proposed SRR process.

pressures, which are determined by each alternative column operating condition. For each column operating condition with a selected column top pressure, given product specification and feed stream information, the parameters for tuning the column are reflux ratio and distillate over feed ratio.

The developed process superstructure is shown in Figure 6. Each column has four candidate operating conditions (varies by pressure, condenser and reboiler duties), among which only one needs to be identified in order to get minimum utility cost over the whole process. Before setting up

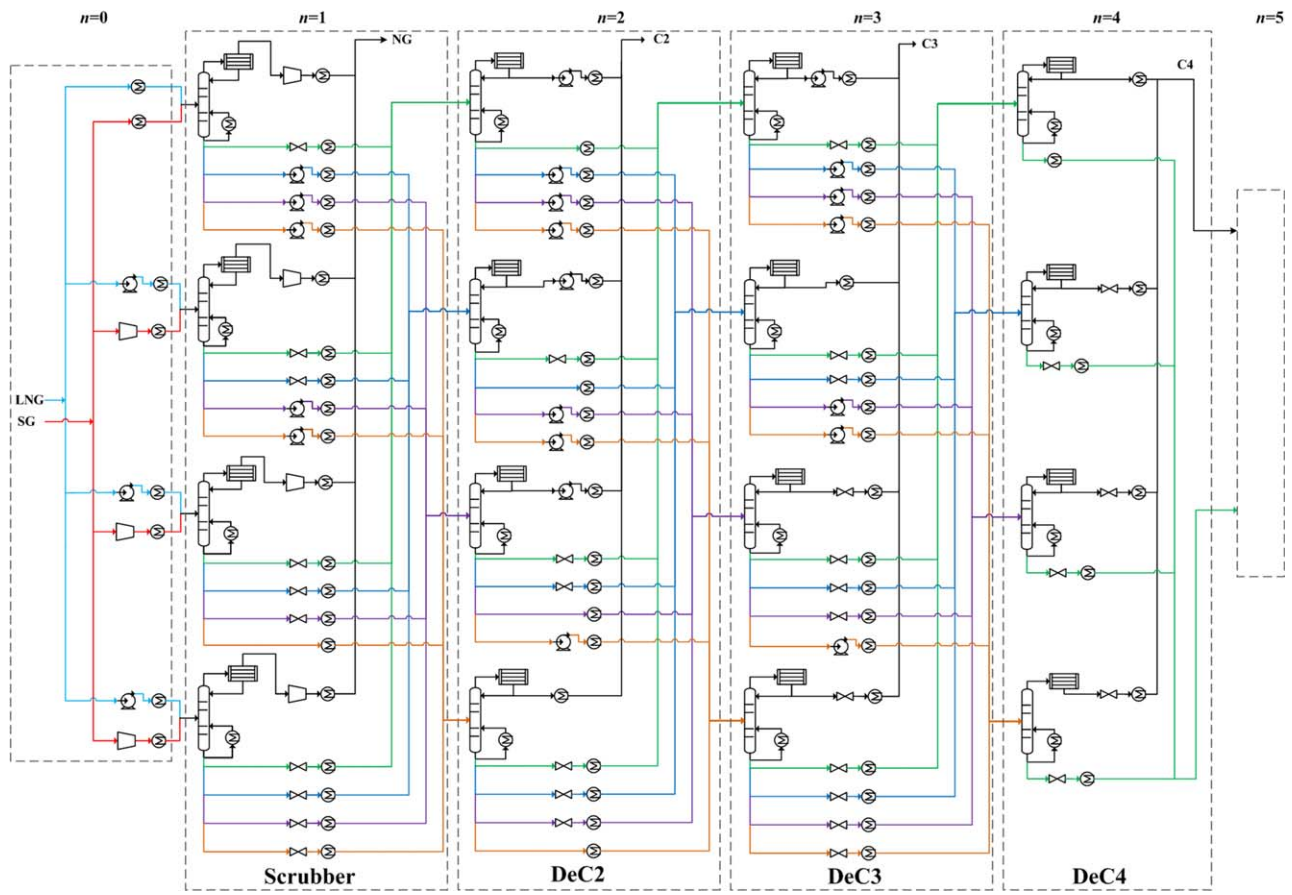

Figure 6. Superstructure of the proposed SRR process.

[Color figure can be viewed in the online issue, which is available at wileyonlinelibrary.com.]

Table 2. Column Design Condition and Specifications

Unit Operating Conditions	Column Bottom Pressure (MPa)				Top Product		Key Variable Recovery Rate
	1	2	3	4			
Scrubber	1	2	3	4	Vapor	7 MPa	99.9%
DeC2	0.75	1.5	2.25	3	Liquid	3 MPa	98%
DeC3	0.75	1.5	2.25	3	Liquid	1.5 MPa	99.9%
DeC4	0.6	1.2	1.8	2.4	Liquid	0.65 MPa	99.9%

the operating conditions of each column, a lot of prior simulations have been performed, and the attempt is to cover a wide range for the operating conditions. The highest pressures are selected to prevent streams entering their supercritical conditions. Also, literature researches have helped identify the lowest pressures for each separation stage. Finally, four different pressure settings are employed from the highest to the lowest pressures with a common pressure difference between two adjacent pressure settings, which causes the total pressure settings to vary by a factor of 4. Note that more pressure settings can be selected, and more selections only will enlarge the modeling and optimization problem size rather than influence any part of the developed methodology. Table 2 indicates the detailed operation information for different columns. To follow ordinary operation routine, the feed to each column will be adjusted to its bubble point at corresponding pressure by passing through necessary units, such as pump, valve, and heat exchanger. For instance, the second candidate condition of DeC2 is operated at 1.5 MPa; and there are four possible feeds from the bottom of the scrubber. Thus, all the possible feeds to DeC2 under its second operating conditions should be processed to its bubble point at the pressure of 1.5 MPa. As indicated in the superstructure, the bottom stream from the first candidate condition of the scrubber needs a pump to increase its pressure, so as to be fed into DeC2; while the other candidate conditions of the scrubber connected to DeC2 at 1.5 MPa need valves to decrease the bottom streams' pressures. Through an optimal synthesis described in the following sections, only one operating condition for each separation unit will be selected, such that the overall utility cost will be the minimum. Note that all the column product specifications are set according to the literature survey.[12]

Also note that once every candidate operating condition of a column is identified, the associated streams of a column that possess heat recovery potentials (e.g., column condenser stream, top product stream, and reboiler stream) as well as the possible connection streams between two adjacent columns can also be known through simulation. Thus, the flow rate and the inlet and outlet temperatures and pressures of all the streams in the superstructure can be obtained before the optimal process and HEN synthesis are conducted. In other words, the heat transfer (heating or cooling) load of each stream in the superstructure, their compression work, and their pump power if applicable can all be calculated through simulations, which will be used as part of the input data for process and HEN synthesis in the next step of work.

In the second step, an MILP model is developed and solved in GAMS[13] in order to identify the optimal process flow sheet. All the necessary information from simulation results, such as condenser and reboiler duties, compressor shaft work, pump power, and heat exchanger duty, are integrated in the MILP model. Based on the superstructure, all the possible process streams along with their starting and ending temperatures will be collected. All these inlet and outlet temperatures help define a series of temperature intervals, which can be used to generate a transshipment model for heat integration optimization.[14] The transshipment model is imbedded into the MILP model. Its objective function is to identify the best operating condition combination from different columns in terms of bearing the minimum total utility cost.

When the optimal operating conditions of all columns have been identified, real connection streams among different columns are also determined. Meanwhile, the target of the minimum utility cost from heat integration is also obtained. In the third step, the HEN design will be conducted to accomplish the minimum utility cost with a detailed network configuration. The final HEN configuration is obtained a manually trial-and-error method according to the pinch design methods.[15] It provides detailed heat exchange relation among those selected process streams.

The final step of this work is to validate the identified SRR process design through rigorous simulations with Aspen Plus. Possible troubleshooting may be performed in early steps of work in case the validation results are not satisfied. Iteratively, a final completed conceptual design for the proposed SRR process, including detailed process configuration and operating information for every unit and stream, will be presented.

Superstructure Development and Data Preparation

Superstructure development

Based on Figure 6, the entire superstructure is divided into several stages. The feeds of LNG and shale gas are classified as stage 0 ($n = 0$); scrubber, DeC2, DeC3, and DeC4 are, respectively assigned from stages 1 through 4; and the downstream process for adopting DeC4 effluents is regarded as the 5th stage in this superstructure. Note that here the 5th stage is introduced to help process stream mapping to generate the transshipment model. It refers to the subsequent processes after the last distillation column. Thus, the total number of stages is six (i.e., $n = 0, 1,\ldots, N$, where $N = 5$). On each stage n, assume there are M_n operating conditions available.

For stage $1 \le n \le 4$, one and only one operating condition will be selected; once an operating condition at that stage is selected, the interconnection streams between any two adjacent stages will also be identified. Two sets of binary variables, x and y, are employed in the developed MILP model, where $x_m^n = 1$ stands for the m-th operating condition at the n-th stage is selected, otherwise $x_m^n = 0$; $y_{m,m'}^{n,n+1} = 1$ means the stream from the m-th operating condition at the n-th stage connecting to the m'-th operating condition at the $(n+1)$-th stage is selected, otherwise $y_{m,m'}^{n,n+1} = 0$. Based on the

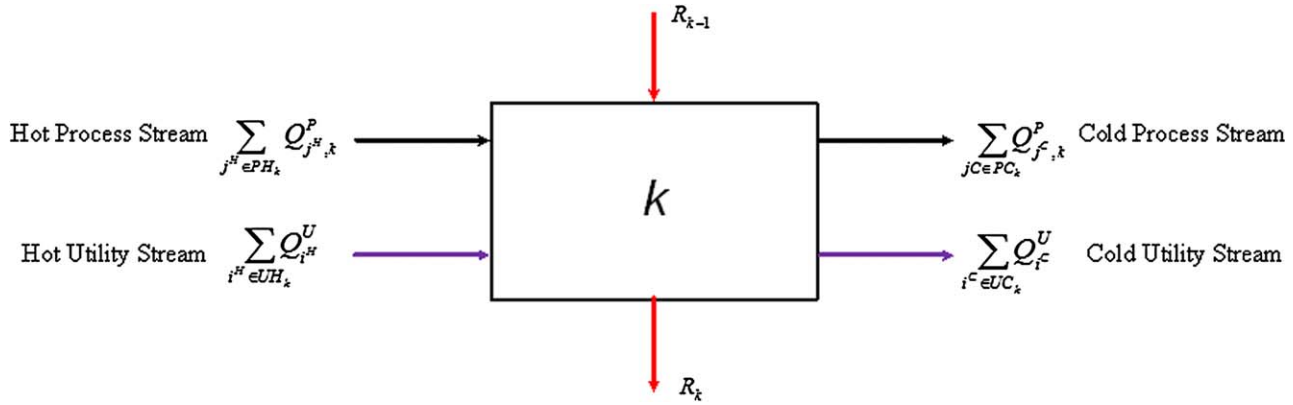

Figure 7. Heat flows in temperature interval *k*.[15]

[Color figure can be viewed in the online issue, which is available at wileyonlinelibrary.com.]

definitions, the logic relations of the superstructure can be expressed as follows

$$\sum_{m \in S_n} x^n_m = 1, \forall n \in \{1, ..., N\} \tag{1}$$

$$x^0_m = 1, \forall m \in S_0 \tag{2}$$

$$\sum_{m' \in S_{n+1}} y^{n,n+1}_{m,m'} = x^n_m, \forall n \in \{0, ..., N-1\}, \forall m \in S_n \tag{3}$$

$$\sum_{m \in S_n} y^{n,n+1}_{m,m'} = x^{n+1}_{m'}, \forall n \in \{1, ..., N\}, \forall m' \in S_{n+1} \tag{4}$$

$$y^{0,1}_{m,m'} = x^1_{m'}, \forall m \in S_0, \forall m' \in S_1 \tag{5}$$

where S_n is the operating condition set for stage n: $\forall S_n \in \{1, ..., M_n\}$. In this study, $\forall M_n = 4$ for $n \in \{1, 2, 3, 4\}$. For the beginning stage $n = 0$, $M_0 = 2$; while for the last stage $n = 5$, $M_5 = 1$. The equations above show the logic relations among related binary variables. They can be explained as follows: for stages with S_n operating conditions ($\forall n \in \{1, ..., N\}$), only one condition will be selected (Eq. 1), while stage 0 has two conditions (LNG and shale gas) that both must be selected (Eq. 2). Equation 3 suggests that if the m-th condition at the n-th stage ($\forall n \in \{0, ..., N-1\}$) is selected (i.e., $x^n_m = 1$), the outlet stream from this condition will feed to one and only one condition in the downstream ($n+1$)-th stage; otherwise, if = 0, there will be no outlet streams from the m-th condition at the n-th stage connecting to the downstream. Similarly, Eq. 6 constrains the relations between x^{n+1}_m and its upstream connection ($y^{n,n+1}_{m,m'}$). Specifically, for stage 0, both conditions of S_0 (i.e., LNG and shale gas) have to feed a selected operating condition, or do not feed to an unselected operating condition at the 1st stage.

Stream Index Mapping and Data Preparation

Stream index mapping

Since heat integration is the main concern for this design, any potential stream that will receive or consume energy (either going through a heat exchanger, a compressor, or a pump) needs to be considered in the optimization model, in order to find an optimal HEN design that will maximize its heat recovery and minimize its operating cost. For the heat integration of all the potential streams appearing in the superstructure in Figure 6, the method of a transshipment model[14] is employed in this article. In the transshipment model, hot streams are treated as source nodes, and cold streams are treated as sink nodes. Heat can be regarded as a commodity that must be transferred from the sources to the sinks through some intermediate "warehouses" that correspond to the temperature intervals that guarantee feasible heat exchange.[16] Note that the transshipment model needs to form a total of K temperature intervals that are based on the inlet and outlet temperatures of all hot and cold streams. Thus, the general heat balance in the k-th temperature interval is represented by Figure 7.

Note that the process streams in Figure 7 are from alternative process streams already indexed based on the stage n and operating condition m from the superstructure (e.g., $y^{n,n+1}_{m,m'} = 1$ means the stream from the m-th operating condition at the n-th stage to the m'-th operating condition at the ($n+1$)-th stage is selected). However, to employ the transshipment model, all the streams indexed based on n and m need to be mapped to a new set of indices suitable for the transshipment model formulation. For this purpose, a general rigorous index mapping method is developed in this article, which is shown in Figure 8.

The idea represented by Figure 8 is to enumerate the number of stages n, operating condition m and m', and column associated streams d (e.g., column condenser stream, top product stream and reboiler stream presented by the superstructure in Figure 6) to develop a new set of index of j. Thus, the index j is a function of n, m, and m', or a function of n, m, and d; meanwhile, the binary value of interconnection stream $y^{n,n+1}_{m,m'}$ and column operating condition x^n_m can be mapped to a newly defined binary of z_j, indicating if the j-th stream is selected ($z_j = 1$) or not selected ($z_j = 0$) by the SRR synthesis. Quantitatively, for the interconnection streams between two stages, their indices j can be mapped by Eq. 10

$$j(n, m, m') = m' + (m-1)(M_{n+1} + \delta_n) + \sum_{e=0}^{n-1} M_e(M_{e+1} + \delta e), \forall m \in S_n, \forall m' \in S_{n+1}, \forall n \in \{0, ..., N-1\} \tag{6}$$

where δ_n is the number of associated column streams at stage n, and not belonging to interstage connection streams (e.g., column condenser stream, top product stream, and reboiler stream). From the superstructure in Figure 6, it suggests

$$\delta_0 = \delta_n = 0 \tag{7}$$

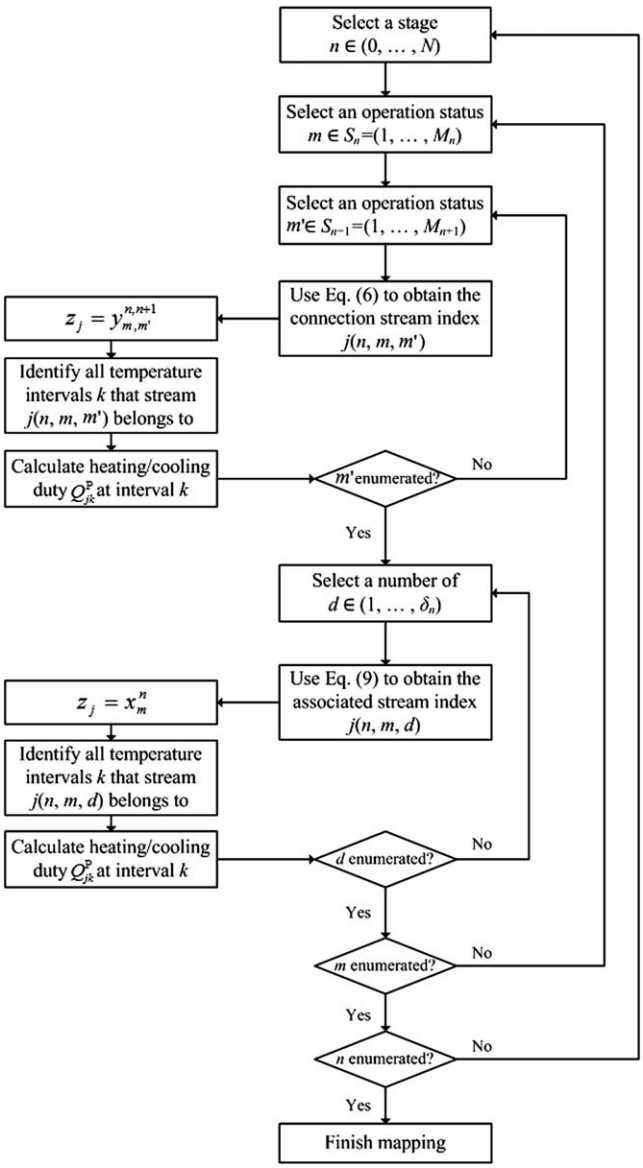

Figure 8. General stream index mapping methodology based on the superstructure.

$$\delta_n=3, \forall n \in \{1, ..., N-1\} \tag{8}$$

To map the indices of the associated column streams at stage n that are not belonging to interstage connection streams, Eq. 17 can be employed. In this study, the associated streams from stage n ($\forall n \in \{1, ..., N-1\}$) are designated as condenser stream ($d = 1$), top product stream ($d = 2$), and reboiler stream ($d = 3$)

$$j(n, m, d)=M_{n+1}+(m-1)(M_{n+1}+\delta_n)+\sum_{e=0}^{n-1} M_e(M_{e+1}+\delta_e) +d, \forall m \in S_n, \forall d \in \{1, ..., \delta_n\}, \forall n \in \{0, ..., N-1\} \tag{9}$$

After the index mapping for every stream in the superstructure, a new binary variable, will be assigned to each stream j to represent if this stream will be selected ($z_j = 1$) or not ($z_j = 0$) during the process synthesis. Through the stream index mapping method, for interstage connection streams, Eq. 10 must hold, while for the column associated streams, Eq. 11 must be satisfied

$$z_j=y^{n,n+1}_{m,m'}, \forall m \in S_n, \forall m' \in S_{n+1}, \forall n \in \{0, ..., N-1\} \tag{10}$$

$$z_j=x^n_m, \forall m \in S_n, \forall n \in \{1, ..., N-1\} \tag{11}$$

Heat load, compressor work, and pump power calculation

Based on the newly mapped stream index, the process data used for optimal SRR synthesis can be developed. As aforementioned, all column candidate operating conditions and process streams in the superstructure can be simulated in advance. Therefore, the heat transfer load (Q_j), possibly involved compression shaft work (W_j), or pump power (HP_j) for every stream j in the superstructure can be calculated through simulations, which are generally represented as

$$Q_j=Q\left(T_j^{in}, T_j^{out}, P_j^{in}, P_j^{out}, \mathbf{C}_j, F_j\right) \tag{12}$$

$$HP_j=HP\left(T_j^{in}, T_j^{out}, P_j^{in}, P_j^{out}, \mathbf{C}_j, F_j\right) \tag{13}$$

$$W_j=W\left(T_j^{in}, T_j^{out}, P_j^{in}, P_j^{out}, \mathbf{C}_j, F_j\right) \tag{14}$$

where functions of $Q(\bullet)$, $HP(\bullet)$, and $W(\bullet)$ stand for simulations with Aspen Plus, which, respectively give, and. Obviously, they are functions of the inlet temperature (T_j^{in}), outlet temperature (T_j^{out}), inlet pressure (P_j^{in}), outlet pressure (P_j^{out}), stream compositions ($\mathbf{C}_j$), and flow rate (F_j) for the j-th stream.

Specifically, to employ the transshipment model for HEN synthesis, the heat load of each stream needs to be allocated to different temperature intervals. According to the simulation results, the inlet and outlet temperatures of all possible process streams help define a temperature array. Any two adjacent temperatures in this temperature array define a temperature interval. Assume there are in total K temperature intervals. For one temperature interval k, the heat flow balance is shown in Figure 7. It includes heat flows from hot and cold process streams and hot and cold utilities, inflow heat residual from the previous interval $k-1(R_{k-1})$, and outflow heat residual to the interval $k+1(R_k)$.

According to the identified temperature intervals, the heat-transfer load of process stream j in the k-th temperature interval can also be identified, which has the quantitative relationship with the total heat-transfer load of Q_j^P as

$$Q_j^P=\begin{cases} \sum_{k=1}^{K} Q^P_{j^H,k}, & \text{if } j \text{ is a hot process stream} \\ \sum_{k=1}^{K} Q^P_{j^C,k}, & \text{if } j \text{ is a cold process stream} \end{cases} \tag{15}$$

where j^H and j^C are, respectively, the index of hot and cold process streams $Q^P_{j^H,k}$ and $Q^P_{j^C,k}$ are, respectively, the heat load that stream j^H inputs to or stream j^C takes away from temperature interval k. Hot process streams are defined as the heat source during heat exchanging, thus their temperatures decrease; while cold process streams extract heat during heat exchanging, and their temperatures increase.

Note that to define temperature intervals in this study, three minimum temperature differences are specified. For streams with temperature under 30°C, the minimum temperature

Table 3. Utility Information

Utility	Temperature (°C)	Cost
HP Steam	185	\$6.68/GJ
LP Steam	148	\$3.11/GJ
Water	32	\$0.159/GJ
Electricity	–	\$0.0805/kWh

difference is set as 2°C; with the temperature between 30 and 40°C, the minimum temperature difference is set as 5°C; while with the temperature above 40°C, 10°C is the minimum temperature difference. The reason for choosing such different values is that the cold energy tends to be more valuable when the heat exchange happened below ambient temperature (30°C is used in this work), and usually the real plant adopts small temperature difference with large-heat exchange areas to accomplish the desired heat exchange; while for higher-temperature streams, a larger temperature difference is applied to the process in order to decrease heat exchanger size, which is related to the capital cost. In this study, there are 108 heat process streams which have defined a total of 197 temperature intervals (some streams have the same inlet or outlet temperatures). Also note that there are four types of utilities used in this design, including electricity and three heating utilities: high-pressure steam, low-pressure steam, water for heating or cooling. Detailed utility information is shown in Table 3.

Synthesis Model Development and Solution Identification

SRR synthesis model development

The employed transshipment model for HEN integration is generalized by Eqs. 16–19. Equation 16 gives the heat balance; Eq. 17 requires the heat residual from every temperature intervals should be nonnegative, which means the heat only flows from a high-temperature interval to a low-temperature interval. Obviously, the heat residuals to the first interval (R_0) and from the last interval (R_K) should both be 0 (Eqs. 18 and 19)

$$R_k - R_{k-1} = \left(\sum_{i^H \in UH_k} Q^U_{i^H} - \sum_{i^C \in UC_k} Q^U_{i^C} \right) + \left(\sum_{j^H \in PH_k} Q^P_{j^H,k} - \sum_{j^C \in PC_k} Q^P_{j^C,k} \right), \forall k \in \{1, ..., K\} \tag{16}$$

$$R_k \geq 0, \forall k \in \{1, ..., K-1\} \tag{17}$$

$$R_0 = 0 \tag{18}$$

$$R_K = 0 \tag{19}$$

where that $Q^U_{i^H}$ is the heat load of the hot utility stream i^{H}; and $Q^U_{i^C}$ is the heat load of the cold utility stream i^{C}. Note that all the variables in Eq. 16 are positive numbers, and the sign ahead of each term is determined according to Figure 7.

The objective of the SRR synthesis model is to minimize the total utility cost (ϕ) as shown in Eq. 20

$$\min_{y^{n,n+1}_{m,m'}, x^n_m} \phi = \sum_{i^H \in UH_k} C^U_{i^H} Q^U_{i^H} + \sum_{i^C \in UC_k} C^U_{i^C} Q^U_{i^C} + \sum_j \left(W_j + HP_j \right) C_E z_j \tag{20}$$

where $C^{\mathrm{U}}_{i^H}$ stands for the unit cost of hot utility $i^H \in$ (water, high-pressure steam, low-pressure steam); stands for the unit cost of cold utility $i^C \in$ (water); C_E is the unit cost of electricity for compressor shaft work and pump power. Equations 1–20 help construct the entire synthesis model. Although it employs previous studies on the transshipment model for HEN integration, it also includes much more new contents such as superstructure representation, column condition selection, and stream index mapping.

Solution identification

In this study, the shale gas composition is based on normalized reported data from Fort Worth basin production wells at Barnett shale plays.[17] Its composition information is shown in Table 4.

The developed MILP model is formulated with GAMS. It contains 572 equations, 535 single variables, and 132 binary variables. The model is solved by the CPLEX solver, which uses a branch and cut algorithm to solve a series of LP, subproblems.[18] The computation time actually takes 0.132 s on Dell Vostro 470, which using Intel® Core(TM) i7–3770 CPU at 3.40 GHz with 4.00 GB RAM. The solution obtained from GAMS for this MILP model is 1347.92 \$/h. The optimal solution for SRR synthesis is shown in Figure 9: selecting the third operating condition for scrubber and DeC2, the first operating condition for DeC3, and the second operating condition for DeC4. The needed heat utilities are low-pressure steam for 7.06 GJ/h, and water as the heating source for 86.52 GJ/h. The electricity consumption is about 16.3 MW.

HEN Configuration and Final Design Validation

Based on the obtained SRR synthesis solution, the target for the maximum internal heat recovery has been obtained. Meanwhile, the number of optimally selected process streams has become one fourth of the original number, since now each stage selected one operating condition out of four assumptions. In the next step, a heat integration design including detailed network configuration should be identified. A completed separation process with selected operating condition and interstage connection streams is simulated to fulfill the HEN design. Table 5 gives the simulation results for all the process streams involved for the combined separation process, which will be used for the final HEN configuration. Based on the stream information from simulation results, now only 32 temperature intervals have left (shown in Figure 10). Figure 10 indicates that the total needed heating utility for the whole process is about 93.61 GJ/h. Compared with the GAMS optimization result of 93.58 GJ/h, there is only 0.03% difference. This demonstrates the efficacy of data preparation in the first step and the developed MILP model.

Figure 10 reveals the heat flow information for all the heat process streams. From the figure, process streams and utilities having heat exchange potentials at certain

Table 4. Shale Gas Composition

Component	Composition (mol %)
Nitrogen	2.82
Methane	86.90
Ethane	6.69
Propane	1.95
Isobutane	0.57
n-Butane	0.77
Isopentane	0.17
n-Pentane	0.14

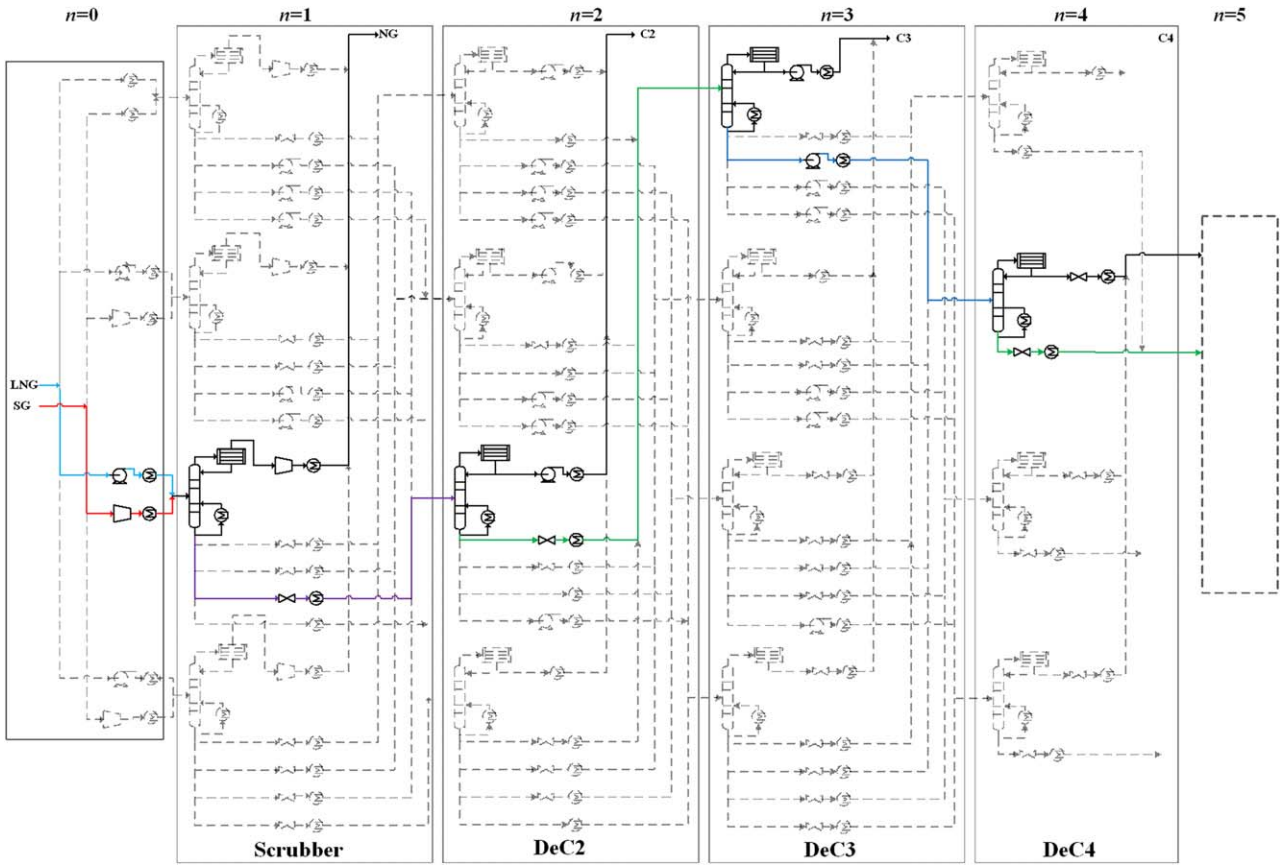

Figure 9. SRR process synthesis results.

[Color figure can be viewed in the online issue, which is available at wileyonlinelibrary.com.]

temperature intervals could be further analyzed. The results show that the actual utilities needed include low-pressure steam for 6.99 GJ/h and water as the heating source for 86.63 GJ/h, while GAMS results indicate 7.03 GJ/h of low-pressure steam and 86.52 GJ/h of water. Note that Figure 10 also suggests the heat residual information from one temperature interval to another. At the interval between 61.46°C to 64.15°C on cold stream temperature, the heat residual become 0, which indicates a Utility Pinch occurs at this temperature interval. The reason that there is zero heat flow in the temperature interval is the use of water as a hot utility is maximized to reduce the amount of LP stream required, since water is relatively cheaper than LP steam. This interval with no heat residual divides the overall HEN into upper and lower sections. The heat composite curves for the entire HEN are plotted in Figure 11, which shows the heat exchange is practical since there is no temperature crossover and the total required hot utility is 93.61 GJ/h.

To highlight the merit of this work, the hot and cold utility independently needed for both LNG regasification and NGL recovery process before integration are also estimated for comparison. For the same amount of LNG and shale gas feed streams, the total hot utility duty will be 244.86 GJ/h and the total cold utility is 151.25 GJ/h, respectively. Compared with this study, the optimal design can save about 61.8% of hot utility and 100% of cold utility.

Based on a manually trial-and-error method, one possible HEN configuration satisfying the thermodynamic matching and heat load presented in Figure 10 is proposed in Figure 12. Euler's Rule in Graph Theory indicates that the number of connections (arcs) U in a graph with N nodes, L loops and S subgraphs: $U = N + L - S$. In pinch analysis, this rule is used for targeting ahead of design, thus, loops and subgraphs are unknown. The common assumption made is that $L = 0$ (since loops can be removed by additional use of energy), and that $S = 1$ (since having subgraphs, $S \geq 2$ would be a positive surprise, not counted for at the targeting stage). As a result, the well know rule for targeting the minimum number of units $U = N - 1$ is developed. At each section

Table 5. Summary of the Final SRR Process Streams

	Stream	Index j	Inlet T (°C)	Outlet T (°C)	ΔH (GJ/h)
	LNG	3	−159.13	−94.85	55.73
	SG	7	129.02	−66.78	−79.11
Scrubber	Top Stream	27	−96.85	−96.98	−32.50
	Bottom Stream	29	7.48	23.66	83.78
	Top Product	28	−43.36	25.00	67.38
	Bottom Product	25	12.24	8.88	−2.43
DeC2	Top Stream	55	−3.91	−6.95	−19.27
	Bottom Stream	57	64.15	75.66	21.81
	Top Product	56	−5.67	5.59	1.36
	Bottom Product	51	31.49	23.11	−3.11
DeC3	Top Stream	69	12.53	7.18	−8.45
	Bottom Stream	71	61.46	64.54	8.98
	Top Product	70	7.89	7.89	0
	Bottom Product	66	64.99	86.14	0.57
DeC4	Top Stream	98	79.81	79.07	−5.18
	Bottom Stream	100	129.02	129.50	5.26
	Top Product	99	50.05	42.00	−0.77
	Bottom Product	97	96.16	42.00	−0.45

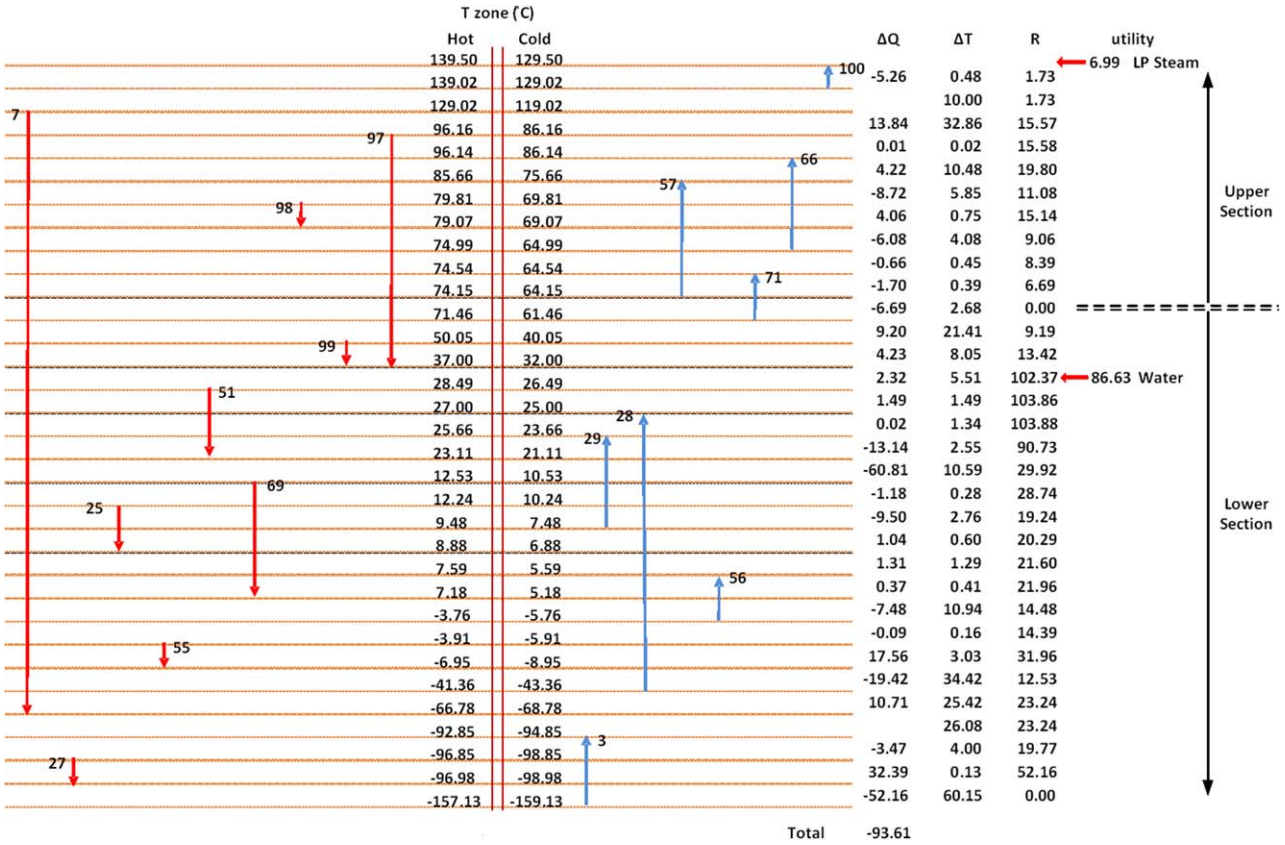

Figure 10. Temperature intervals for the SRR process.

[Color figure can be viewed in the online issue, which is available at wileyonlinelibrary.com.]

above and below utility pinch point, the number of heat exchangers reaches the minimum number based on Euler's rule in graph theory, which is equal to the number of nodes (consisted of heat process streams (N^{P}) plus the number of utilities (N^{U}) in this work) minus one (see Eq. 21). In the aforementioned section the utility pinch point, there are seven heat process streams and one utility stream; thus, seven heat exchangers are used. In the following section the utility pinch point, there are 12 heat process streams and one utility, 12 heat exchangers are employed

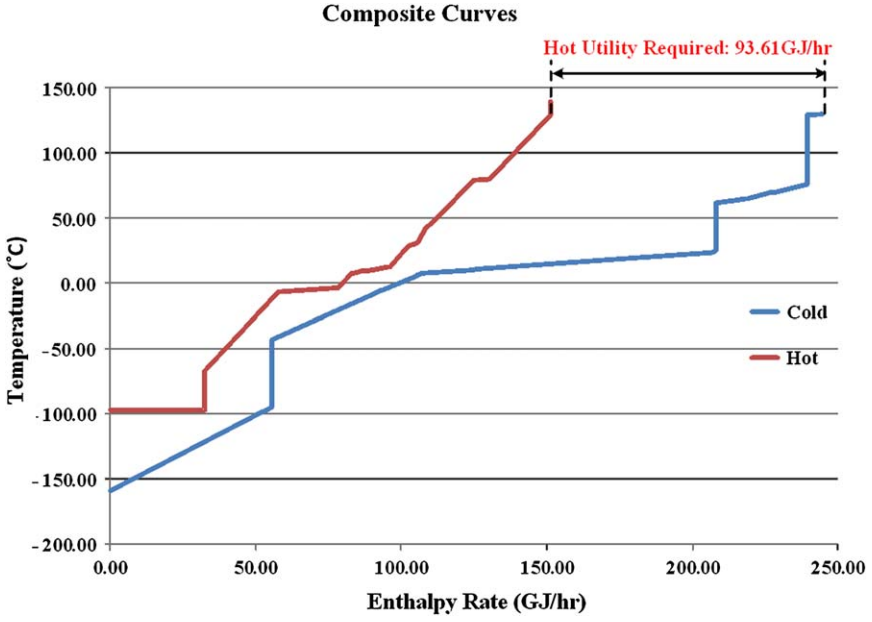

Figure 11. Composite curves of the SRR process.

[Color figure can be viewed in the online issue, which is available at wileyonlinelibrary.com.]

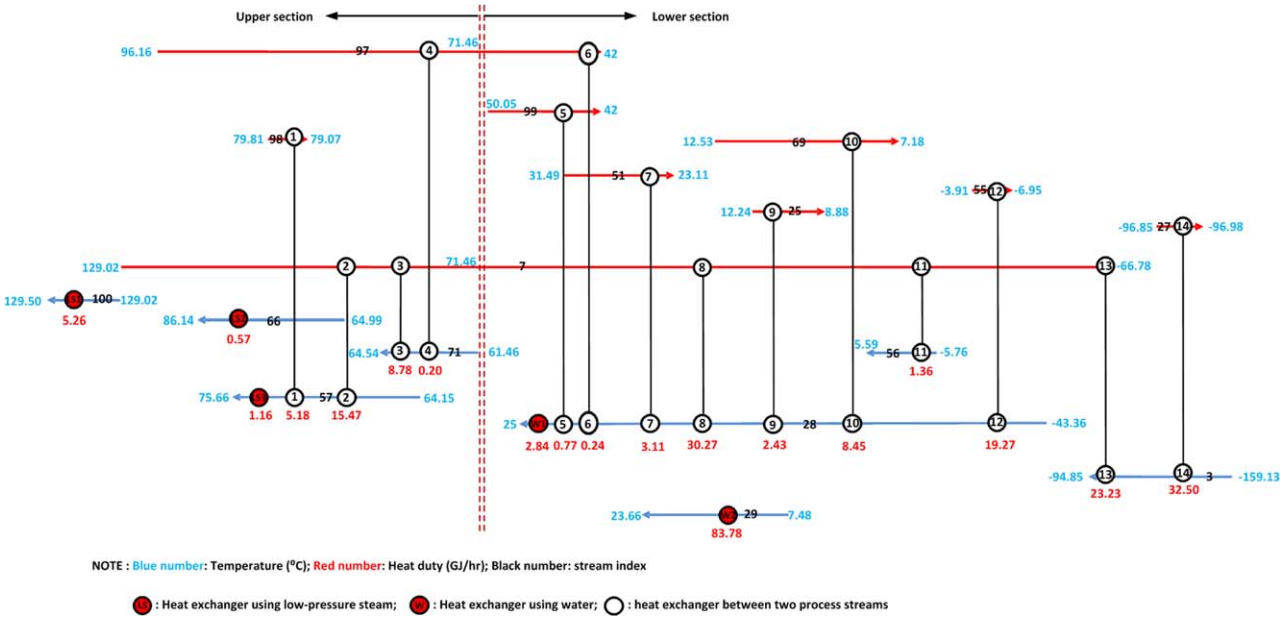

Figure 12. Heat exchange network configuration for matches.

[Color figure can be viewed in the online issue, which is available at wileyonlinelibrary.com.]

$$N_{\min} = N^{P} + N^{U} - 1 \tag{21}$$

According to the last step of the proposed methodology framework, a plant-wide rigorous simulation with Aspen Plus is conducted to examine the integrated separation and HEN of the SRR process. The validation results show that the proposed conceptual SRR design works perfectly. Figure 13 shows the validated results, where the process flow sheet and major operating condition of each unit and stream such as temperature and pressure are all disclosed.

Concluding Remarks

In this work, a novel conceptual design is developed based on a systematic methodology for an LNG receiving terminal. Because an LNG regasification process consumes a lot of hot energy as well as performing NGL recovery from shale gas and LNG to obtain more valuable products needs a large amount of cold energy, this novel design integrates shale gas NGL recovery with LNG regasification processes, so that a win-win situation can be accomplished by exchanging both available hot and cold energy internally, which results in great economic benefits on energy savings. In the developed systematic methodology, rigorous simulation, MILP based process synthesis, and HEN design and configuration are coupled together for generating the integrated SRR process. A case study has demonstrated the efficacy of the developed methodology and the conceptual SRR design.

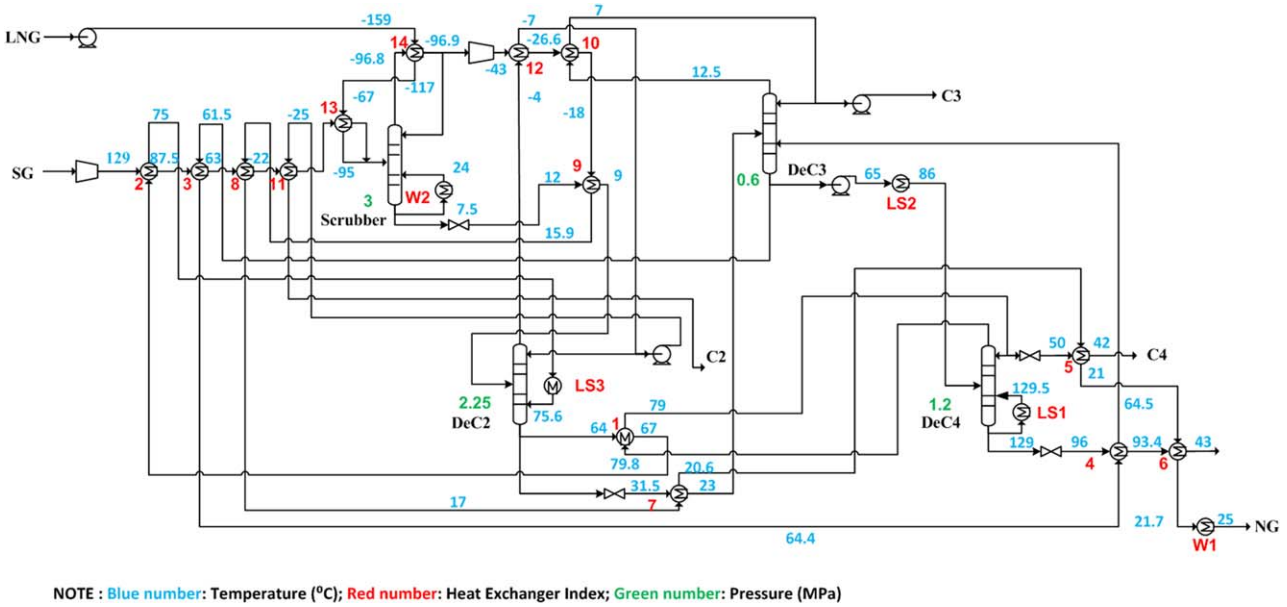

Figure 13. Validated SRR process configuration with operating conditions.

[Color figure can be viewed in the online issue, which is available at wileyonlinelibrary.com.]

Acknowledgments

This work was supported in part by Texas Air Research Center, Texas Hazardous Waste Research Center, and Graduate Student Scholarship from Lamar University.

Notation

Sets and indices

i = index of utility stream
i^C = index of cold utility stream
i^H = index of hot utility stream
j = index of process stream
j^C = index of cold process stream
j^H = index of hot process stream
k = index of temperature interval
m = index of operating condition
n = index of process stages
PH_k = index set of hot process streams associated with the k-th temperature interval
PC_k = index set of cold process streams associated with the k-th temperature interval
S_n = set of operating condition at the n-th stage
UH_k = index set of hot utility streams associated with the k-th temperature interval
UC_k = index set of cold utility stream associated with the k-th temperature interval

Parameters

$C^U_{i^H}$ = unit cost of hot utility i, \$/GJ
$C^U_{i^C}$ = unit cost of cold utility i, \$/GJ
C_E = cost of electricity, \$/kWh
K = total temperature intervals
δ_n = number of the associated column streams at stage n not belonging to interstage connection streams

Variables

F = mass flow rate, kg/h
HP = pump power, GJ/h
$N_{\min}$ = the minimum number of heat exchangers
N^P = number of process streams
N^U = number of utilities
P = pressure, MPa
Q^P_j = the heat load that process stream j supplies or demands, GJ/h
$Q^U_{i^H}$ = the heat load of hot utility stream i^H, GJ/h
$Q^U_{i^C}$ = the heat load of cold utility stream i^C, GJ/h
$Q^P_{j^H,k}$ = the heat load that hot process stream j^H inputs to temperature interval k, GJ/h
$Q^P_{j^C,k}$ = the heat load that cold process stream j^C takes away from temperature interval k, GJ/h
R_k = heat residual from temperature interval k, GJ/h
T = temperature, °C
W = compressor shaft work, GJ/h
x, y, z = binary variables
ϕ = total utility cost

Functions

$Q(\bullet)$ = heat-transfer load from rigorous simulation
$W(\bullet)$ = compressor shaft work from rigorous simulation
$HP(\bullet)$ = pump power from rigorous simulation

Literature Cited

1. EIA. US crude oil, natural gas, and NG liquids proved reserves 2010. Available online at http://www.eia.doe.gov/oil_gas/natural_gas/data_publications/crude_oil_natural_gas_reserves/cr.html. Accessed March 29, 2011.
2. BP p.l.c., BP Statistical Review of World Energy; June 2012.
3. Kinnaman TC; The economic impact of shale gas extraction: A review of existing studies. *Ecol Econ*. 2011;70:1243–1249.
4. Continental Economics, Inc.; The Economic Impacts of US Shale Gas Production on Ohio Consumers; January 2012. Available online at http://www.eidohio.org/wp-content/uploads/2012/02/Economic-Impacts-of-Shale-Gas-Production_Final_23-Jan-2012.pdf.
5. EIA. United States shale gas maps 2011. Available online at http://www.eia.gov/pub/oil_gas/natural_gas/analysis_publications/maps/maps.htm. Accessed May 20, 2012.
6. FERC, Available online at http://www.ferc.gov/industries/lng.asp. Accessed September 17, 2012.
7. Liu CW, Zhang J, Xu Q, Gossage JL. Thermodynamic-analysis-based design and operation for boil-off gas flare minimization at LNG receiving terminals. *Ind Eng Chem. Res*. 2010;49:7412–7420.
8. Trocquet B. Adding value to LNG through NGL Recovery. LNG North America Summit. *Mustang Engineering*; June 2008.
9. Ortloff Engineers, Ltd., NGL/LPG recovery for LNG. Ortloff LNG Fractionation Brochure. 2007.
10. Cuellar KT, Hudson HM, Wilkinson JD. Economical options for recovering NGL/LPG at LNG receiving terminals. The 86th Annual Convention of The Gas Processors Association; March 2007.
11. AspenTech, Inc. Aspen Physical Property System - Physical Property Methods, version 7.1: Cambridge, MA; May 2011.
12. The Linde Group. Natural gas processing plants. 2010. Available online at http://www.linde-india.com/userfiles/image/File/Natural%20Gas%20Processing%20Plants.pdf, accessed September 20, 2012.
13. GAMS. GAMS Development Corp.: Washington, DC; November 2009.
14. Papoulias SA, Grossman IE. A structural optimization approach to process synthesis - II. Heat recovery network. *Comput Chem Eng*., 1983; 7:707–721.
15. Linnhoff B., Hindmarsh E.The pinch design method for heat exchanger networks. *Chem Eng Sci*. 1983;38(5):745–763.
16. Biegler LT, Grossmann IE, Westerberg AW. *Systematic Methods of Chemical Process Design*. Saddle River, NJ: Prentice Hall PTR; 1997.
17. Hill RJ, Jarvie DM, Zumberge J, Henry M. Pollastro RM. Oil and gas geochemistry and petroleum systems of the Fort Worth basin. *AAPG Bulletin*. 2007;91:445–473.
18. GAMS. *The Solver Manuals*. GAMS Washington, DC: Development Corp; November 2009.

Manuscript received Nov. 30, 2012, revision received July 3, 2013, and final revision received Sept. 10, 2013.